Simulations of an etched spiral axial attenuation scheme for an on-axis reflecting telescope

Aaron Spector, Guido Mueller

Department of Physics, University of Florida

Abstract

The current generation of proposed space based interferometric gravitational wave detectors all use a reflecting telescope to transfer the laser signals between the space- craft. One of the proposed telescope designs is an on-axis classical Cassegrain with the secondary mirror axially aligned to the primary mirror. Since the outgoing beam will be incident normal to the secondary, some of the light will be reflected directly back to the optical bench. Length changes between the telescope structure and the optical bench will cause this back-reflected light to introduce phase noise to the measuremen t signal. The phase noise from this process must be suppressed below 0.1 μcycles / $\sqrt{\text{Hz}}$ to meet the LISA requirements. We have presented simulations that demonstrate that the back-reflected power can be sufficiently attenuated by using a specifically patterned Anti-Reflective (AR) region, in the shape of a spiral, at the center of the secondary mirror.

1 Introduction

While the specific design of the first generation of space-based interferometric gravitational-wave detectors remains uncertain, all of the proposed missions use reflecting telescopes to transfer laser signals between Spacecraft (SC) separated by vast distances [1] [2]. One concern with using an on-axis telescope, like the one seen in Figure 1a, is that light will be directly back-reflected to the optical bench from the telescope secondary mirror. This light can have phase noise that will couple into the measurement signal due to the length fluctuations in the distance between the telescope and the optical bench. Using the Laser Interferometer Space Antenna (LISA) requirements on technical noise sources as a guide, our goal is to suppress the back-reflection induced phase noise below 0.1 μcycles/$\sqrt{\text{Hz}}$. To achieve this we must cast a shadow along the optical axis of the telescope and reduce the spatial overlap between the field received from the far SC and the back-reflected field. The spatial overlap (η), as defined in [3], is a measure of the interferometric contrast between these two fields evaluated over the area of the photodetector on the LISA optical bench. For length changes of 10 nm/$\sqrt{\text{Hz}}$ between the telescope structure and the optical bench η

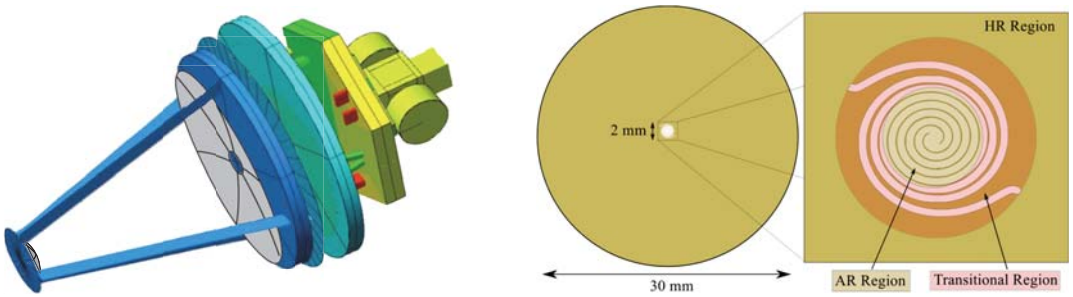

(a) On-axis telescope **(b)** Etched secondary and spiral pattern

Figure 1: (a) Mock design for an on-axis telescope in blue and optical bench in yellow. (b) Secondary with a gold HR coating and spiral pattern (unwound by a factor of 1000) etched into its center. White is representative of the etched region exposing the substrate.

must be less than 5×10^{-6}. If no axial attenuation scheme is present the unmitigated spatial overlap between these fields is 3×10^{-4} [3]. This means that the total back-reflected power in the spatial mode of the received field must be attenuated by 3.5 orders of magnitude.

2 Axial Attenuation with Sub-wavelength Etching

While it is possible to attenuate the axial back-reflection using a discrete Anti-Reflective (AR) region at the center of the secondary, it is difficult to reduce the spatial overlap below the LISA requirements due to light scattering from the edge of the AR region. This has motivated us to pursue coatings that use a smooth transition in the reflectivity from the Highly Reflective (HR) region to the AR region. Our previous work suggested that a sinusoidal rolloff between these regions will prevent diffraction effects from scattering light back along the optical axis of the telescope [3].

One way to obtain this transition in the reflectivity is to etch sub-wavelength features into a metallic HR coating such as gold. Doing this forms an effective index between the HR coating and the substrate that varies according to the surface density of gold at a given point on the mirror. We can then tune the surface density across the mirror to get a spatially dependent reflectivity. With a spiral etching pattern, like the one shown in Figure 1b, the surface density depends on how tightly the spiral is wound. In the center of the spiral, the AR region, the surface density of gold is set so that an equal power of light is reflected from the gold and the exposed fused silica substrate. Since the gold layer is a quarter-wave thick these two fields destructively interfere. The spiral in Figure 1b is unwound by a factor of 1000 to show its shape. In reality, the spiral will not only be much more tightly wound, but the width of the gold ridges will be on the order of hundreds of nm.

As the radius of the pattern gets larger, the spiral begins to unwind and the surface

density of gold increases thus causing an increase in the reflectivity of that point on the mirror. This smooth rise in the reflectivity forms the transitional region between the AR and HR regions. Once the HR region is reached, the spiral ends and the surface of the substrate is entirely covered in gold. While any reflective metallic coating could be used, our theoretical analysis will focus on gold because of its high reflectivity of 98% at 1064 nm and our familiarity with etching it.

3 Spiral Design

The first step in designing the spiral was making the reflectivity of the AR region as low as possible. As mentioned earlier, this was done by adjusting the surface density and thickness of the gold coating such that the light reflected from the gold destructively interferes with the light reflected from the area where the substrate is exposed. By doing a superposition of the field reflected from fused silica with the field reflected from the gold we found the following equation for the effective reflectivity R_{e_o} in the AR region. Here d represents the thickness and S_{Au_o} is the surface density of gold. The first term, $S_{Au_o}\left(\frac{1-N_{Au}}{1+N_{Au}}\right)$, represents the coefficient of reflection for the portion of the incident field reflected from the gold. The second term is the coefficient of reflection for the portion of the field reflected by the exposed fused silica. The surface density of fused silica in the AR region, $1 - S_{Au_o}$, is multiplied by the coefficient of reflection of fused silica, with N_{Si} being the complex index of refraction of fused silica. It is then multiplied by an additional phase factor due to the thickness of the gold coating.

$$R_{e_o} = \left| S_{Au_o}\left(\frac{1-N_{Au}}{1+N_{Au}}\right) + (1-S_{Au_o})\left(\frac{1-N_{Si}}{1+N_{Si}}\right)e^{-i\frac{2\pi}{\lambda}2d}\right|^2 \tag{1}$$

λ is the laser wavelength of 1064 nm. For gold deposited on a fused silica substrate we found that the ideal thickness is 243 nm and the ideal surface density of the gold is 16%.

Next we found the following equation for the axial angle ϕ of the spiral as a function of its radius r in the AR region. Here w is the width of the trenches in the gold coating that expose the substrate and comprise the spiral.

$$\phi_{AR}(r) = \frac{2\pi}{w}(1-S_{Au_o})r \tag{2}$$

As the radius increases the axial angle increases linearly to maintain a constant spacing between the trenches. This keeps the surface density of gold at 16% to preserve the AR properties of this region.

With the spiral defined for the AR region the next step was to unwind the spiral to achieve the appropriate rolloff in the transitional region. As the spiral goes to larger radii the spacing between the trenches grows. This gradually increases the surface density of the metallic coating and produces the rolloff in R_e. In our case we have chosen a Hanning

window function rolloff shown in the following equation due to its success in our original paper [3].

$$R_e(r) = \frac{1 - \cos\left(\pi \frac{r-a}{b-a}\right)}{2} \tag{3}$$

Using the rolloff in equation 3 we came up with the following equation for the spiral in the transitional region.

$$\phi_{trans}(r) = \frac{(1 - S_{Au_o})}{w} \left(\pi r + (b-a)\sin\left(\pi \frac{r-a}{b-a}\right)\right) \tag{4}$$

This equation continuously increases the spacing between the trenches as the spiral get larger to achieve a rolloff in the effective reflectivity shown in equation 3. Also, when $r = a$ the axial angle of the spiral is the same in equation 2 and 4 to ensure that the spiral is continuous at the interface between the AR region and the transitional region. This equation for $a < r < b$, with equation 2 for $r \leq a$, define the entire spiral.

4 Simulations

Simulations for the back-reflected distribution from the spiral were done by calculating the Huygen's integral at an object plane on the secondary for each point along a grid that defined the image plane at the input of the optical bench. Here the field calculated from the Huygen's integral was then subtracted from an expression for the propagated TEM_{00} mode. The resulting distribution was then propagated through the rest of the optical train to the location of the photodetectors using an FFT propagation script [4]. Once we had the distribution at the photodetectors we evaluated the spatial overlap between the resulting field and a simulated field received from the far SC.

5 Results

The simulated back-reflected distribution from the spiral gave a spatial overlap at the photodetector of $2{\times}10^{-7}$, demonstrating that the spiral pattern was able to reduce the mode matched power by more than 6 orders of magnitude. This comfortably exceeded the 3.5 orders of mode matched power attenuation needed to suppress the spatial overlap below the 5×10^{-6} requirements.

The resulting intensity distribution of the spiral back-reflection can be seen in Figure 2a. The unmitigated back-reflection had a relatively flat intensity distribution of roughly 20 W/m^2. The back-reflected distribution from the spiral pattern had an intensity of 6.7×10^{-5}W/m^2 on the optical axis, which was nearly 5.5 orders of axial intensity suppression. The peak intensity shown in the spiral's back-reflected distribution was 0.012 W/m^2, or 3.2 orders of intensity suppression. This bright region, however, makes up a relatively

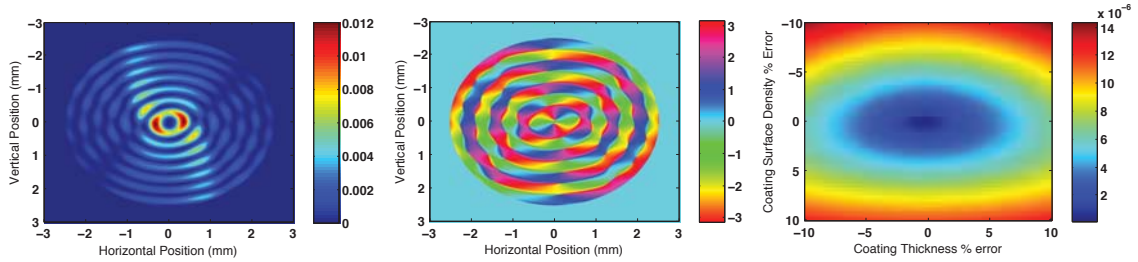

(a) Spiral back-reflection **(b)** Back-reflected phase **(c)** Coating error tolerances

Figure 2: (a) Simulated back-reflected intensity distribution from a spiral etched mirror apertured by the collimating mirror of the telescope (W/m^2). (b) Simulated phase of the back-reflection from a spiral etched mirror with the wavefront curvature removed (radians). (c) Results from a simulation on the effect of errors in the coating thickness and surface density in terms of η evaluated over the detector.

small portion of the distribution. In fact, the total power suppression was 4.2 orders of magnitude when integrating over the entire distribution seen in Figure 2a and 4.0 orders of magnitude when evaluating over the area incident on the photodetector. This would be sufficient to meet the requirements even without considering the phase of the back-reflected distribution which further attenuated the mode matched power.

Figure 2b displays the phase of the back-reflected distribution with the spherical wavefront curvature removed. From this image the spatial incoherence of the back-reflected field is quite apparent. Since the field received from the far SC has a relatively flat wavefront this will help further suppress the spatial overlap as different regions of back-reflected distribution will produce different phases that will destructively in the interference beatnote with the received field at the photodetector. This destructive interference accounted for the remaining two orders of magnitude suppression in the mode matched power.

It is important to point out that this can all be done without any additional AR coating on the substrate since the etched gold coating itself is anti-reflective. In addition to this, the tolerances on the thickness and surface density of the gold coating are realistically achievable. Figure 2c shows result of simulating the spatial overlap at the photodetector with errors in the thickness and surface density of the gold coating. Even with $\pm 4\%$ errors in the coating surface density and $\pm 7\%$ errors in the coating thickness the spatial overlap will still be suppressed below the 5×10^{-6} requirement. Our conversations with manufacturers suggest that coatings with these specifications should be attainable. The results of these simulations show that etching an AR spiral pattern into a metallic coating is a viable method for sufficiently attenuating the axial back-reflection below the LISA requirements.

References

[1] Oliver Jennrich. "LISA technology and instrumentation". In: *Classical and Quantum Gravity* 26.15 (2009), p. 153001. URL: http://stacks.iop.org/0264-9381/26/i=15/a=153001.

[2] Jeff Livas. *SGO Mid: A LISA-Like Concept for the SGO at a Middle Cost Point*. URL: http://pcos.gsfc.nasa.gov/studies/gravwave/gravitational-wave-mission-rfis.php.

[3] Aaron Spector and Guido Mueller. "Back-reflection from a Cassegrain telescope for space-based interferometric gravitational-wave detectors". In: *Classical and Quantum Gravity* 29.20 (2012), p. 205005. URL: http://stacks.iop.org/0264-9381/29/i=20/a=205005.

[4] H Yamamoto et al. "Simulation tools for future interferometers". In: *Journal of Physics: Conference Series* 32.1 (2006), p. 398. URL: http://stacks.iop.org/1742-6596/32/i=1/a=061.

[5] Aaron Spector and Guido Mueller. "Experimental investigation of the back-reflection from an on-axis telescope for space-based interferometric gravitational-wave detectors". In: *to be published* (2014).